Cardiovascular abnormalities with normal blood pressure in tissue kallikrein-deficient mice

Pierre Meneton*†, May Bloch-Faure*, Albert A. Hagege‡, Hartmut Ruetten§, Wei Huang*, Sonia Bergaya¶, Debbie Ceiler*, Doris Gehring§, Isabelle Martins*, Georges Salmon*, Chantal M. Boulanger¶, Jürg Nussberger∥, Bertrand Crozatier**, Jean-Marie Gasc††, Didier Heudes‡‡, Patrick Bruneval‡‡, Tom Doetschman§§, Joël Ménard*, and François Alhenc-Gelas*

*Institut National de la Santé et de la Recherche Médicale (INSERM) U367, 17 Rue du Fer à Moulin, 75005 Paris, France; ‡Faculté de Médecine Necker-Enfants Malades, Université Paris V, 156 Rue de Vaugirard, 75015 Paris, France; §Aventis, Disease Group Cardiovascular, Building H821, 65926 Frankfurt a.M., Germany; ¶INSERM U541, 41 Boulevard de la Chapelle, 75010 Paris, France; ∥Division of Hypertension, Hôpital Universitaire, CH-1011 Lausanne, Switzerland; **INSERM U400, Faculté de Médecine, 8 Rue du Général Sarrail, 94000 Créteil, France; ††INSERM U36, 3 Rue d'Ulm, 75005 Paris, France; ‡‡INSERM U430, Hôpital Broussais, 96 Rue Didot, 75014 Paris, France; and §§Department of Molecular Genetics, Biochemistry, and Microbiology, University of Cincinnati College of Medicine, Cincinnati, OH 45267-0524

Tissue kallikrein is a serine protease thought to be involved in the generation of bioactive peptide kinins in many organs like the kidneys, colon, salivary glands, pancreas, and blood vessels. Low renal synthesis and urinary excretion of tissue kallikrein have been repeatedly linked to hypertension in animals and humans, but the exact role of the protease in cardiovascular function has not been established largely because of the lack of specific inhibitors. This study demonstrates that mice lacking tissue kallikrein are unable to generate significant levels of kinins in most tissues and develop cardiovascular abnormalities early in adulthood despite normal blood pressure. The heart exhibits septum and posterior wall thinning and a tendency to dilatation resulting in reduced left ventricular mass. Cardiac function estimated *in vivo* and *in vitro* is decreased both under basal conditions and in response to β-adrenergic stimulation. Furthermore, flow-induced vasodilatation is impaired in isolated perfused carotid arteries, which express, like the heart, low levels of the protease. These data show that tissue kallikrein is the main kinin-generating enzyme *in vivo* and that a functional kallikrein–kinin system is necessary for normal cardiac and arterial function in the mouse. They suggest that the kallikrein–kinin system could be involved in the development or progression of cardiovascular diseases.

Various endocrine, paracrine, and neuronal peptide systems control blood pressure and cardiovascular function. Active kinins are liberated from kininogens after cleavage by proteases and bind locally to two types of receptors, B1 and B2, which are involved in various functions including vasodilatation, ion epithelial transport, smooth muscle contraction, cell proliferation, and nociception (1, 2). From a cardiovascular viewpoint, the kallikrein–kinin system is thought to antagonize the effects of the renin–angiotensin system. The functional coupling between the two systems is illustrated by the angiotensin I-converting enzyme whose two active sites are able to generate angiotensin II from angiotensin I and to degrade kinins into inactive peptides (3). This tight coupling has precluded a clear demonstration whether the antihypertensive and cardioprotective effects of angiotensin I-converting enzyme inhibitors are solely related to the inhibition of angiotensin II production or also to the inhibition of kinin degradation (4).

In addition to tissue kallikrein, many proteases including plasma kallikrein, trypsin, plasmin, cathepsins, calpains, and some serine proteases encoded by the tissue kallikrein gene family have been shown to be able to generate kinins *in vitro* (5–8). However, the physiologically relevant kinin-forming enzymes have not been clearly established *in vivo* largely because of the lack of specific inhibitors. Several arguments suggest that tissue kallikrein may play an important role. The expression of the gene depends highly on environmental factors such as potassium and sodium dietary intakes (9–12), which are known

to have important cardiovascular and blood pressure effects. Low urinary excretion levels of tissue kallikrein have been linked to the risk of developing hypertension in both humans and rodents (13–16). In addition, mice and hypertensive rats chronically or transiently overexpressing the human tissue kallikrein gene present hypotension (17–19). Tissue-kallikrein-deficient mice were created to investigate directly the role of the protease *in vivo*. The lack of tissue kallikrein abolishes the kinin-forming capacity in most tissues and induces cardiac and vascular abnormalities, with no change in blood pressure.

Materials and Methods

Generation of Tissue Kallikrein-Deficient Mice. The targeting vector was constructed by using two mKlk1 gene fragments of 1.4 kb (*Eco*RI-*Sac*I) and 2 kb (*Bsg*I-*Hind*III) isolated from a mouse 129/Sv phage library (20). The neomycin-resistance gene, replacing a region of 100 bp (*Sac*I-*Bsg*I) in exon 4, was used for selecting R1 embryonic stem cells together with the herpes simplex virus/thymidine kinase gene that was linked to the extremity of the 2-kb genomic fragment. Electroporation and selection of embryonic stem cells and blastocyst-mediated transgenesis were performed as described previously (21). The PCR primers used for the diagnostic analyses of targeted embryonic stem cell clones and for the genotyping of mice were in intron 3 (5′-TGGGTCTTCTCCAAGCAACAGAGAG-3′), intron 4 (5′-GAAGGATGCAAAGAGCCTGCCTAGC-3′), and the neomycin-resistance gene (5′-GCATGCTCCAGACTGC-CTTG-3′).

Northern Blot, Reverse Transcription (RT)-PCR, and Immunohistochemistry. Total RNA and Northern blots were prepared by conventional methods (22) and hybridized with a 0.4-kb tissue kallikrein cDNA probe spanning nucleotides 159–549. RT-PCR (annealing temperature 68°C; 35 cycles) was performed with primers situated in exon 2 (5′-GCTTCACCAAATATCAATGT-GGGGGTATC-3′) and exon 4 (5′-CACACTGGAGCT-CATCTGGGTATTCAT-3′) for mKlk1, and with primers located in exon 4 (5′-CATATACGAACCCGCAGATGA-TCTCCAGTG-3′) and exon 5 (5′-CTTTTATCCAAGAGTTA-AACTTAATAAGTTTG-3′) for mKlk5. The organs were perfused *in vivo* with paraformaldehyde before paraffin embedding and immunostaining with an anti-rat tissue kallikrein antibody (23), which was revealed by immunoperoxidase detection

---

(biotinylated anti-rabbit IgG and ABC complex; Vector Laboratories).

Kinin-Forming Activity and Bradykinin Assays. Tissue kallikrein activity was assessed by measuring the generation of kinins with an RIA after incubation with an excess of semipurified bovine kininogen (24). Tissues first were perfused with modified Hank's solution, homogenized in Tris·HCl buffer (pH 8.5), and solubilized with 1% (mass/vol) deoxycholic acid. Urine and feces were collected by using individual metabolic cages (Marty Technologie, Marcilly-Sur-Eure, France) over 24-h periods, and the feces were homogenized in 0.75 M nitric acid. Endogenous bradykinin was measured by RIA after tissue homogenization in ethanol, subsequent solid-phase extraction on phenylsilylsilica, followed by isocratic reversed-phase HPLC on dodecylsilylsilica using methanol/0.1% phosphoric acid as a mobile phase (25).

Blood Pressure and Heart Rate Measurements. Nonanaesthetized mice, warmed at 30°C, were trained daily for 1 week for restrainers and tail-cuff inflation. Systolic blood pressure and heart rate then were recorded daily (20 determinations in a row) over a 2-day period by using a PowerLab/S system connected to CHART software (A. D. Instruments, Milford, MA). Each determination was individually examined before being included in the final data set.

Morphometric and Histological Analyzes. Hearts were arrested at diastole by injection of potassium chloride and fixed by perfusion at diastolic pressure with 5% (vol/vol) formalin and 0.1 mg/ml sodium nitroprusside and by overnight immersion in 10% (vol/vol) formalin. For each heart, two transversal sections 5-μm thick encompassing the whole left ventricle were cut, embedded in paraffin, and stained with hematoxylin/eosin for histological analysis. For morphometric measurements, each section was stained with Sirius red and scanned with a calibration of 15 μm per pixel (Sony 3 charge-coupled device camera). Left ventricular dimensions were determined with an image analyzer (Nachet NS 15000, Nachet-Vision, les Ulis, France; ref. 26). For each parameter, the final values were the mean of the values measured on the two sections.

Echocardiography. Transthoracic measurements were performed on anaesthetized mice (ketamine/xylazine). We used a Sequoia ultrasound device (Acuson, Mountain View, CA) equipped with a specifically designed 13–15 MHz short-focus linear array probe (15L8; ref. 27). Two-dimensional guided M-mode images were obtained perpendicular to the ventricular septum and posterior wall at the tip of the mitral valve leaflets. End diastolic and systolic left ventricular (LV) diameter as well as septum and posterior wall thickness were measured by using the American Society of Echocardiography leading-edge method. From these parameters, fractional shortening was calculated as [(LV diameter$_{diastole}$ − LV diameter$_{systole}$)/LV diameter$_{diastole}$] × 100 and left ventricular mass as [(septum thickness$_{diastole}$ + LV diameter$_{diastole}$ + LV posterior wall thickness$_{diastole}$)^3 − (LV diameter$_{diastole}$)^3] × 1.04.

Assessment of Left Ventricular Function in Vivo. Anaesthetized mice (thiopental/ketamine) were intubated and ventilated (Hugo Sachs Elektronics, Frieburg, Germany) with a 1:1 mixture of oxygen and room air, and a tidal volume of 10 μl/g of body weight at 140 breaths per min. The left ventricle was catheterized through the right carotid artery by using a miniaturized impedance catheter (Millar Instruments, Houston, TX) to measure simultaneous pressure–volume relationship (28). For absolute volume measurements, the catheter was calibrated with known volumes of heparin-treated mouse blood, using special calibration tubes. Calibrated values were corrected by subtraction of the parallel conductance (conductance of surrounding structures of the cavity) measured by hypertonic injection [10 μl of 15% (vol/vol) saline] into the external jugular vein. The calibration factor used to compensate for nonuniform intracardiac electric field was set at 1. Pressure–volume signals were measured at steady state by a catheter introduced into the right jugular vein. Data were digitized with a sampling rate of 1,000 Hz and recorded with specialized software (HEM; Notocord, Croissy-Sur-Seine, France) before analysis of pressure–volume loops with PVAN software (Millar Instruments).

Assessment of Left Ventricular Function in Isolated Work-Performing Hearts. After excision, hearts were immediately perfused at 37.5°C and at constant pressure of 60 mmHg (1 mmHg = 133 Pa) in a retrograde fashion through the aorta with modified Krebs buffer gassed with 95% O_2/5% CO_2. A catheter was passed through the pulmonary vein into the left ventricle, pulled through the ventricular wall, anchored in the apex by a fluted end, and connected to a tip-micromanometer (1.4 French; Millar Instruments). The left atrium was cannulated through the same pulmonary vein. Hearts were switched to the working mode with constant preload and afterload pressures of 10 and 60 mmHg, respectively, and allowed to stabilize for 30 min. Aortic outflow and atrial inflow were measured continuously by using ultrasonic flow probes (HSE/Transonic Systems, Ithaca, NY). All hemodynamic data were digitized at a sampling rate of 1,000 Hz and recorded by specialized software (HEM).

Calcium Transients and Shortening in Isolated Cardiomyocytes. Cardiomyocytes were isolated from hearts perfused 10 min with 0.8 mg/ml collagenase solution using a Langendorff column (29). After 2 h of incubation allowing adhesion of the cells on laminin, cardiomyocytes were preloaded with indo 1/AM, a fluorescent calcium dye that can freely diffuse across cell membrane. Measurements were carried out by dual-emission fluorimetry with the mean emission 405/480 nm ratio of each cell being used as an index of free cellular calcium. Electrical pacing was performed at a frequency of 1 Hz. Cardiomyocyte shortening was measured by video edge detection of the cells.

Measurement of Flow-Induced Dilatation in Isolated Perfused Carotid Arteries. Right carotid arteries (approximately 7 mm in length) were excised and maintained at 37°C in modified Krebs–Ringer solution gassed with 95% O_2/5% CO_2. The arteries were cannulated at both extremities and perfused such that flow and pressure could be modified independently (30). Artery outer diameter, determined with a binocular loop connected to a video camera, and perfusion pressure were continuously recorded by using ACQKNOWLEDGE 881(MP100WS) software (Biopac System, Les Ulis, France). The arteries were equilibrated for 45 min at a transmural pressure of 70 mmHg and a luminal flow rate of 10 μl/min. Changes in outer diameter after step-increases in luminal flow rate were evaluated in arteries precontracted by 10^{-6} M phenylephrine. Passive diameter was measured at termination after incubation of the arteries for 40 min in Ca^{2+}-free control solution containing 2 mM EGTA and 0.1 mM nitroprusside.

Results

The mouse tissue kallikrein gene has been disrupted by replacing 100 bp of exon 4 with the neomycin-resistance gene (Fig. 1A). As shown by Southern blot analysis (Fig. 1B), 4 of 227 selected G418 and gancyclovir-resistant embryonic stem cell clones were correctly targeted. Four chimeric males, issued from the injection of two independent embryonic stem cell clones into C57BL/6 blastocysts, demonstrated transmission of the mutation to the offspring. The two mouse strains thus obtained were bred separately until the phenotype of the homozygous mice was proven to be identical at the molecular and biochemical levels (data not shown). Breeding of heterozygous mice led to wild-
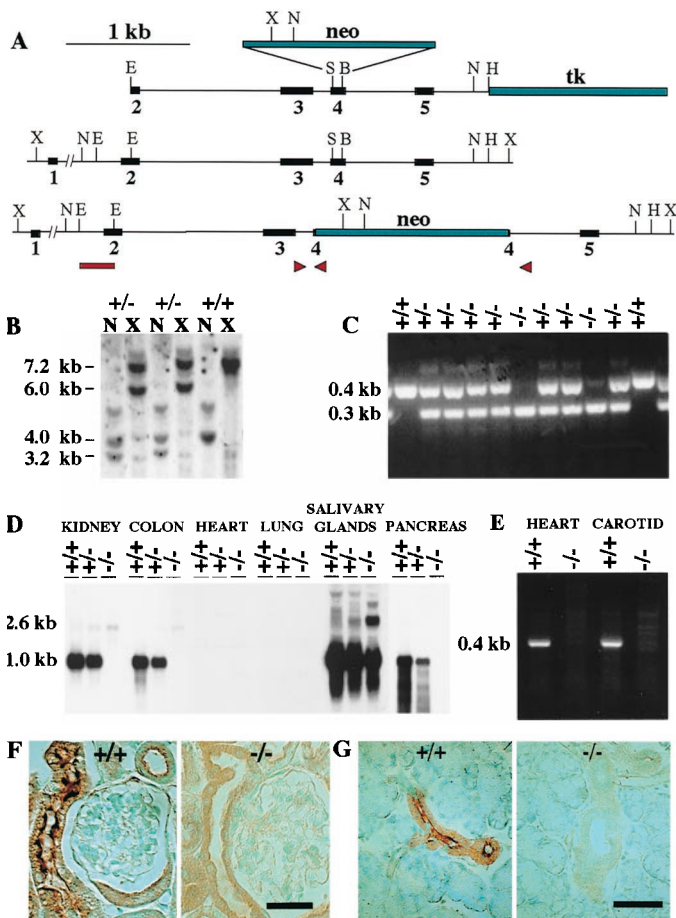
Fig. 1. Targeted disruption of the mouse tissue kallikrein gene. (*A*) The targeting construct containing the neomycin-resistance gene (neo) and the herpes simplex virus/thymidine kinase gene (tk) is shown next to the wild-type and targeted alleles. X, *Xba*I; N, *Nco*I; E, *Eco*RI; S, *Sac*I; B, *Bsg*I; H, *Hind*III. (*B*) Southern analysis of genomic DNA from wild-type (+/+) and targeted (+/−) embryonic stem cells with a probe overlapping intron 1 and exon 2 (bar) reveals different *Nco*I (3.2 versus 4.0 kb) and *Xba*I (6.0 versus 7.2 kb) fragments in the targeted cells. (*C*) PCR analysis of tail DNA from wild-type (+/+), heterozygous (+/−), and homozygous (−/−) mice from offspring of a heterozygous cross, using primers in introns 3 and 4 and in the neo gene (arrowheads in *A*). (*D*) Northern analysis of total RNA (20 µg per lane) from pooled tissues of five +/+, five +/−, and five −/− mice. The blot was hybridized with a mouse tissue kallikrein cDNA probe spanning exons 2 and 3, and was exposed for 6 h. (*E*) Detection of tissue kallikrein mRNA by RT-PCR in the heart and carotid of +/+ mice. The reactions were performed with primers situated in exons 2 and 4, using the same RNA pools that had been used for Northern analysis. The identity of the 0.4-kb band detected in +/+ mice was confirmed to be tissue kallikrein by direct sequencing. (*F*) Immunostaining of tissue kallikrein in the kidneys. The labeling in +/+ mice is localized in the apical membrane of connecting tubular cells. (*G*) Immunostaining of tissue kallikrein in the salivary glands. The labeling in +/+ mice is found in the apical membrane of the epithelial cells lining the excretory ducts. (Bars = 20 µm.)

type (TK$^{+/+}$), heterozygous (TK$^{+/-}$), and homozygous mutant (TK$^{-/-}$) offspring (where TK is tissue kallikrein) with classical Mendelian ratios (137 +/+, 259 +/−, 136 −/−; Fig. 1*C*). All of the analyses have been made on 3- to 4-month-old F$_2$ littermate females harboring a mixed 129/Sv-C57BL/6 genetic background.

Northern analysis of various tissue RNAs shows the absence of the 1-kb tissue kallikrein mRNA in the kidneys, colon, and pancreas of TK$^{-/-}$ mice (Fig. 1*D*). In the salivary glands, the remaining 1-kb band likely corresponds to crosshybridization of

the probe to mRNAs transcribed from the highly homologous members of the tissue kallikrein gene family that are known to be expressed in this tissue (31). The 2.6-kb band observed in organs of TK$^{+/-}$ and TK$^{-/-}$ mice corresponds to tissue kallikrein mRNA harboring the neomycin-resistance gene as demonstrated by specific probe hybridization (data not shown). Tissue kallikrein mRNA levels are very low in the heart and carotid and cannot be detected by Northern analysis. The presence of tissue kallikrein mRNA in these two organs, and its absence in TK$^{-/-}$ mice, can be revealed only by RT-PCR (Fig. 1*E*). Corroborating the absence of the mRNA, tissue kallikrein is undetectable by immunohistochemistry in the kidneys and salivary glands of TK$^{-/-}$ mice, in contrast to TK$^{+/+}$ mice where the protease can be easily identified (Fig. 1 *F–G*).

Measurement of kinin-forming activity in organs and bodily fluids shows an almost complete lack of activity in TK$^{-/-}$ mice and a half reduction in TK$^{+/-}$ mice when compared with TK$^{+/+}$ mice (Table 1). Significant kinin-forming activity still is present in salivary glands, indicating that some members of the kallikrein gene family code for active kinin-forming enzymes. Nevertheless, tissue kallikrein represents by far the main enzyme responsible for the generation of kinins in salivary glands as in the other organs. The absence of endogenous bradykinin in TK$^{-/-}$ mice points to tissue kallikrein as the major enzyme able to generate significant levels of kinins in healthy organs *in vivo* (Table 1). In the heart, kinin-forming activity and bradykinin levels are below the detection limit in all mice independently of the genotype.

Although systolic blood pressure is not modified by the lack of kallikrein (134.3 ± 4.3 versus 125.7 ± 3.6 mmHg in TK$^{+/+}$ mice; $P = 0.19$), cardiac function is abnormal in TK$^{-/-}$ mice. Left ventricular fractional shortening assessed by echocardiography is decreased in TK$^{-/-}$ mice as compared with TK$^{+/+}$ mice (Fig. 2*A*). Given that left ventricular lumen diameter (Fig. 3*A*) and perimeter (Fig. 3*B*) are not significantly different between TK$^{+/+}$ and TK$^{-/-}$ mice, stroke volume is correspondingly reduced in TK$^{-/-}$ mice (16.7 ± 1.9 versus 24.3 ± 1.1 µl; $P < 0.004$) as illustrated in Fig. 2*B*. As TK$^{+/+}$ and TK$^{-/-}$ mice have similar heart rates (648 ± 14 versus 647 ± 15 beats per minute; $P = 0.95$), cardiac output is likewise compromised in TK$^{-/-}$ mice *in vivo* (Fig. 2*C*) and in isolated work-performing hearts (9.7 ± 0.4 versus 11.1 ± 0.4 ml/min; $P < 0.04$). The reduced cardiac output in TK$^{-/-}$ mice is most likely the consequence of left ventricular dysfunction as evidenced from the decreased stroke work (1,132 ± 209 versus 2,028 ± 145 mmHg·µl; $P < 0.004$) and the reduced maximum pressure developments (Fig. 2*D*) and maximal power (Fig. 2*E*) observed *in vivo*. The depressed cardiac contractile phenotype of TK$^{-/-}$ mice also is demonstrated by the reduced systolic pressure (Fig. 2*G*) and external power (data not shown) reached respectively at high afterload and preload pressure values in isolated work-performing hearts. Furthermore, cardiac response to acute β-adrenergic stimulation is depressed in TK$^{-/-}$ mice as compared with TK$^{+/+}$ mice as shown by the smaller increase of fractional shortening after acute dobutamine treatment (Fig. 2*F*).

The histological organization of the myocardium in TK$^{-/-}$ mice appears normal with no indication of myofibrillar disarray, fibrosis, necrosis, or inflammation (data not shown). However, a thinning of the septum and left ventricular posterior wall is evidenced in TK$^{-/-}$ mice by echocardiography (Fig. 3*A*) and histomorphometry measurements (Fig. 3*B*), resulting in a reduced left ventricular mass as the left ventricle is not significantly enlarged (Fig. 3*A*). Calcium cycling, as reflected by diastolic (0.93 ± 0.08 versus 0.94 ± 0.02; $P = 0.97$) and systolic (1.10 ± 0.07 versus 1.08 ± 0.04; $P = 0.81$) cytosolic calcium levels (405/480 nm ratio), and systolic shortening (3.04% ± 0.96% versus 4.31% ± 0.91%; $P = 0.37$) are similar in cardiomyocytes isolated from TK$^{+/+}$ and TK$^{-/-}$ mice.

Table 1. Kinin-forming activity and endogenous bradykinin level in organs and fluids of TK$^{+/-}$ and TK$^{-/-}$ mice as compared with TK$^{+/+}$ mice

Strain	Kinin-forming activity							Endogenous bradykinin	
	pg of BK/h per μg of protein					ng of BK/min per 24-h excretion		fmol/g of tissue	
	Kidneys, n = 7	Colon, n = 7	Pancreas, n = 15	Salivary glands, n = 7	Heart, n = 7	Urine, n = 6	Feces, n = 14	Kidneys, n = 16	Heart, n = 16
+/+	32.6 ± 6.1	32.7 ± 11.5	5,077 ± 1,364	518,743 ± 114,978	1.6 ± 1.1	2,384 ± 164	1,708 ± 452	9.2 ± 1.4	<X
+/−	12.3 ± 2.4	11.6 ± 5.3	1,846 ± 805	118,800 ± 19,697	0.8 ± 0.6	887 ± 173	958 ± 334	NM	NM
−/−	1.2 ± 0.4	1.8 ± 1.0	14 ± 2	7,629 ± 1,856	1.2 ± 0.4	10 ± 1	17 ± 2	2.1 ± 0.5	<X
P	0.0001	0.02	0.0008	0.0001	0.56	0.0001	0.002	0.0001	NA

The detection limit X of endogenous bradykinin (BK) was 1.3 fmol/g of tissue. Values (means ± SEM) have been compared by ANOVA. NM, not measured; NA, not applicable.

In addition to the cardiac defects, an altered vascular reactivity can be detected in TK$^{-/-}$ mice. Indeed, flow-dependent but not acetylcholine-induced vasodilatation is impaired in perfused carotid arteries isolated from TK$^{-/-}$ mice as compared with those isolated from TK$^{+/+}$ mice (Fig. 2H).

Discussion

In all mammalian species studied so far, the tissue kallikrein gene belongs to a family of clustered genes encoding serine proteases and exhibiting very high sequence similarity (32). Gene targeting methods were used to disrupt the mouse tissue kallikrein gene on chromosome 7 (mKlk1, previously named mGK6; ref. 20). Despite the presence of the other members of the gene family, the efficiency of the homologous recombination events was similar to what is habitually obtained for single gene, i.e., 4 targeted embryonic stem cell clones of 227 clones surviving the G418 and gancyclovir selection. Three different arguments indicate that the other genes of the family have not been disrupted and that their expression is not profoundly perturbed. First, restriction profiles performed with five different enzymes are identical in the four targeted embryonic stem cell clones with no indication of chromosomal rearrangement in a 25-kb region, containing at least two other members of the gene family, in the immediate vicinity of the tissue kallikrein gene (data not shown). Second, in the salivary glands, the remaining 1-kb Northern band observed in TK$^{-/-}$ mice is attributable to crosshybridization of the probe with mRNAs encoded by the other members of the tissue kallikrein gene family, which are all expressed in this tissue (31). The decrease intensity of the remaining 1-kb band in TK$^{-/-}$ mice is mainly attributable to the lack of tissue kallikrein mRNA whose expression can be estimated by the intensity of the 2.6-kb band, whereas the expression of the other genes remains approximately the same as that in TK$^{+/+}$ mice. Third, mKlk5, the closest gene present immediately upstream of the tissue kallikrein gene and transcribed in the same direction, appears to be similarly expressed in the salivary glands of TK$^{+/+}$ mice and TK$^{-/-}$ mice as assessed by RT-PCR (data not shown).

No tissue kallikrein mRNA is detected in the kidneys, colon, and pancreas of TK$^{-/-}$ mice, and a half reduction is observed in the organs of TK$^{+/-}$ mice as expected. The lack of functional mRNA encoding tissue kallikrein is confirmed by immunohistochemistry data that show a complete absence of the protease in the kidneys and salivary glands. The almost total disappearance of kinin-forming activity in TK$^{-/-}$ mice (96.3% in the kidneys, 94.5% in the colon, 99.7% in the pancreas, 98.5% in salivary glands, 99.6% in urine, and 99.0% in the feces) indicates that tissue kallikrein is the main enzyme generating kinins *in vivo*. This finding is confirmed by the absence of detectable endogenous bradykinin in the kidneys of TK$^{-/-}$ mice. Thus, the other enzymes suspected to be involved in the generation of kinins, notably plasma kallikrein and the serine proteases encoded by the tissue kallikrein gene family (5, 8), do not seem to participate significantly in the process in most organs. However, it remains to be established whether these enzymes play a role in kinin formation during pathological conditions such as inflammation or infection.

The availability of a kinin-free mouse model is important to decipher the physiological role of the kallikrein–kinin system. Defined phenotypes already have been demonstrated in B2- or B1-receptor-deficient mice. Inactivation of the B2-receptor gene provokes salt-sensitive hypertension (33, 34), altered nociception (35), and reduced urine-concentrating ability (36). Mice lacking the B1 receptor exhibit hypoalgesia and altered inflammatory response (37). However, because of the close proximity of the two genes on chromosome 12, it is unlikely that the breeding of the two mouse strains will easily provide mice lacking both receptors in the near future. In addition, the unexpected existence of two genes encoding kallikrein-sensitive kininogens in the mouse (P.M., unpublished data) will certainly delay the generation of kininogen-free mice as well.

Blood pressure is not significantly different between TK$^{+/+}$ and TK$^{-/-}$ mice even though the decrease in renal and urinary kallikrein activity in TK$^{-/-}$ mice reproduces the phenotype that repeatedly has been associated with hypertension in human and rat studies (13–15, 38). This finding suggests that low renal kallikrein synthesis is not a primary cause of high blood pressure but rather a consequence of hypertension and/or of the associated kidney defects. Nevertheless, it is possible that TK$^{-/-}$ mice harboring different genetic backgrounds or exposed to some environmental conditions known to influence blood pressure, such as high-sodium or low-potassium dietary intakes, may develop hypertension.

The most obvious phenotype of TK$^{-/-}$ mice is the abnormal structure and function of the heart. Tissue-kallikrein-deficient mice present early in adulthood a thinning of left ventricular walls and a diminished left ventricular mass. These structural abnormalities are accompanied by a reduced cardiac function that can be evidenced under basal conditions or during acute β-adrenergic stimulation. This cardiac dysfunction does not seem to result from an intrinsic cardiomyocyte defect as suggested by the normal left ventricular function at low afterload and preload pressure values and by similar calcium cycling and systolic shortening in isolated cardiomyocytes from TK$^{+/+}$ and TK$^{-/-}$ mice. The histological organization of the myocardium in TK$^{-/-}$ mice also seems normal with no indication of myofibrillar disarray, fibrosis, necrosis, or inflammation. In these conditions, the decreased cardiac function in TK$^{-/-}$ mice is most simply explained by the reduced left ventricular mass and the thinner left ventricular walls, which would be unable to develop an adequate contractile force. Such a normal histological architecture of the myocardium associated to a cardiac dysfunction has been described in stunned myocardium phenotype (28) but is in
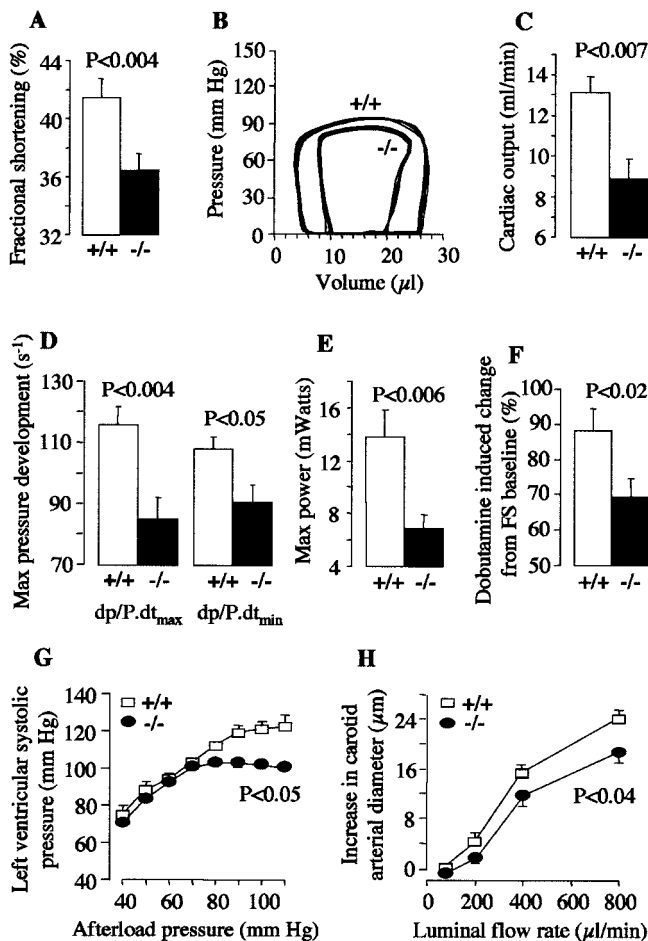
Fig. 2. *In vivo* and *in vitro* assessment of left ventricular function and carotid artery reactivity in TK$^{+/+}$ and TK$^{-/-}$ mice. (*A*) Fractional shortening determined by two-dimensional echocardiography in TK$^{+/+}$ ($n = 25$) and TK$^{-/-}$ ($n = 20$) mice of identical body weight (25.65 ± 0.52 versus 25.63 ± 0.44 g). (*B–E*) Dynamic cardiac parameters measured at steady state with an impedance catheter in TK$^{+/+}$ ($n = 7$) and TK$^{-/-}$ ($n = 6$) mice. (*F*) Cardiac response to acute β-adrenergic stimulation in the same animals used for the determination of baseline fractional shortening. Fractional shortening (FS) was measured before and 10 min after intraperitoneal injection of dobutamine (4 μg/g of body weight). (*G*) Left ventricular function curve determined in work-performing hearts isolated from TK$^{+/+}$ ($n = 5$) and TK$^{-/-}$ ($n = 5$) mice and perfused with a fixed preload pressure of 10 mmHg. (*H*) Effect of luminal flow rate on the outer diameter of carotid arteries isolated from TK$^{+/+}$ ($n = 7$) and TK$^{-/-}$ ($n = 6$) mice. The initial artery diameter precontracted by phenylephrine and the final passive diameter were identical between TK$^{+/+}$ and TK$^{-/-}$ mice (482 ± 10 versus 500 ± 12 μm) and (552 ± 6 versus 562 ± 11 μm), respectively. Diameter was also comparable between TK$^{+/+}$ and TK$^{-/-}$ mice in arteries exposed to 10^{-6} M acetylcholine (536 ± 8 versus 543 ± 11 μm). Values (means ± SEM) have been compared by ANOVA.

Fig. 3. Cardiac structural features of TK$^{+/+}$ and TK$^{-/-}$ mice. (*A*) Two-dimensional echocardiography parameters determined in TK$^{+/+}$ ($n = 25$) and TK$^{-/-}$ ($n = 20$) mice. (*B*) Histomorphometric cardiac dimensions measured on perfusion-fixed hearts isolated from the same animals at termination. The mean body weight was identical between TK$^{+/+}$ and TK$^{-/-}$ mice (25.65 ± 0.52 versus 25.63 ± 0.44 g). Values (means ± SEM) have been compared by ANOVA.

sharp contrast to the myocyte disarray, necrosis, and/or fibrosis observed in hypertrophic or dilated cardiomyopathies (39–41). The cardiac abnormalities of TK$^{-/-}$ mice are reminiscent of those observed in some forms of hypokinetic mildly dilated cardiomyopathy (42, 43), but an exact corresponding phenotype is yet to be found in humans.

These data show that a paracrine regulatory system directly controlled by environmental factors, and not only the compo-
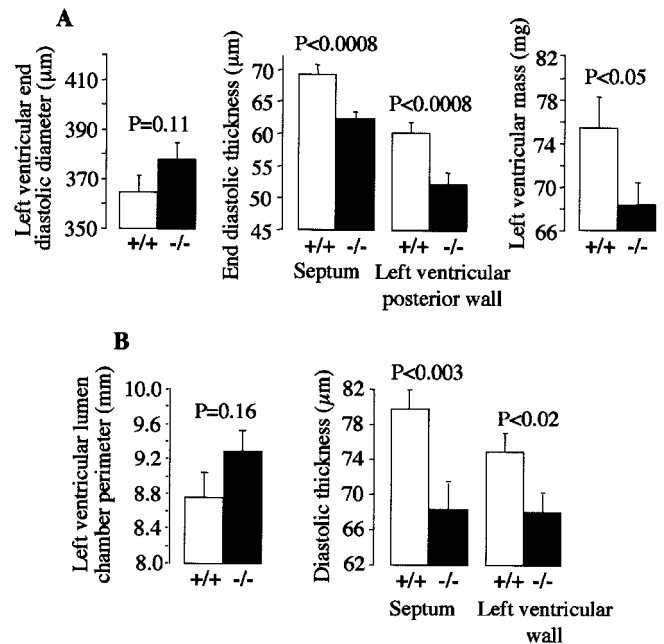
nents of sarcomeres and cytoskeleton (44, 45), can play a significant role in the maintenance of normal cardiac structure and function. The exact mechanisms by which the heart becomes abnormal in TK$^{-/-}$ mice remain to be established. The phenotype might be a direct consequence of the absence of tissue kallikrein in blood vessels. Indeed, the observation that the protease plays an important role in flow-dependent induced dilatation through locally generated kinins, as demonstrated in the carotid artery (46), brings the possibility that the growth deficit of left ventricular walls in TK$^{-/-}$ mice could result from an altered function of the coronary arteries. Alternatively, kinins also may exert a direct trophic effect on the cardiomyocytes through the B2 receptor as suggested recently by *in vitro* and *in vivo* studies (47). Finally, we cannot exclude that the lack of tissue kallikrein in excretory organs may induce systemic disturbances participating to the development of the cardiac phenotype even though no evidence of electrolytic unbalance was found under basal conditions in TK$^{-/-}$ mice (data not shown).

Tissue-kallikrein-deficient mice provide a kinin-free mouse model that should be useful for investigating the role of kinins in many different biological functions and the existence of potential kinin-independent effects of tissue kallikrein. The cardiac phenotype of these mice together with the data recently obtained in transgenic rats overexpressing human tissue kallikrein in the heart (19) raise the possibility that the tissue kallikrein gene, like the B2-bradykinin-receptor gene (48), could be involved in the development or progression of cardiovascular diseases.

1. Carretero, O. A. & Scicli, A. G. (1995) in *Hypertension: Pathophysiology, Diagnosis, and Management*, eds. Laragh, J. H. & Brenner, B. M. (Raven, New York), 2nd Ed., pp. 983–999.
2. Bhoola, K. D., Figueroa, C. D. & Worthy, K. (1992) *Pharmacol. Rev.* **44,** 1–80.
3. Erdos, E. G. (1990) *Hypertension* **16,** 363–370.
4. Linz, W., Wiemer, G., Gohlke, P., Unger, T. & Scholkens, B. A. (1995) *Pharmacol. Rev.* **47,** 25–49.
5. Gapanhuk, E. & Henriques, O. B. (1970) *Biochem. Pharmacol.* **19,** 2091–2096.

6. Ogloblina, O. G., Ruanet, V. V., Kazakova, O. V., Paskhina, T. S. & Orekhovich, V. N. (1980) *Biokhimiya* **45,** 2217–2224.

7. Higashiyama, S., Ishiguro, H., Ohkubo, I., Fujimoto, S., Matsuda, T. & Sasaki, M. (1986) *Life Sci.* **39,** 1639–1644.

8. Hosoi, K., Tsunasawa, S., Kurihara, K., Aoyama, H., Ueha, T., Murai, T. & Sakiyama, F. (1994) *J. Biochem. (Tokyo)* **115,** 137–143.

9. Vio, C. P. & Figueroa, C. D. (1987) *Kidney Int.* **31,** 1327–1334.

10. el-Dahr, S., Yosipiv, I. V., Muchant, D. G. & Chevalier, R. L. (1996) *Am. J. Physiol.* **270,** F425–F431.

11. Hunt, S. C., Hasstedt, S. J., Wu, L. L. & Williams, R. R. (1993) *Hypertension* **22,** 161–168.

12. Hunt, S. C., Wu, L. L., Slattery, M. L., Meikle, A. W. & Williams, R. R. (1993) *Am. J. Hypertens.* **6,** 226–233.

13. Margolius, H. S., Geller, R., Pisano, J. J. & Sjoerdsma, A. (1971) *Lancet* **2,** 1063–1065.

14. Margolius, H. S., Geller, R., De Jong, W., Pisano, J. J. & Sjoerdsma, A. (1972) *Circ. Res.* **30,** 358–362.

15. Berry, T. D., Hasstedt, S. J., Hunt, S. C., Wu, L. L., Smith, J. B., Ash, K. O., Kuida, H. & Williams, R. R. (1989) *Hypertension* **13,** 3–8.

16. Pravenec, M., Kren, V., Kunes, J., Scicli, A. G., Carretero, O. A., Simonet, L. & Kurtz, T. W. (1991) *Hypertension* **17,** 242–246.

17. Wang, J., Xiong, W., Yang, Z., Davis, T., Dewey, M. J., Chao, J. & Chao, L. (1994) *Hypertension* **23,** 236–243.

18. Wang, C., Chao, L. & Chao, J. (1995) *J. Clin. Invest.* **95,** 1710–1716.

19. Silva, J. A., Jr., Araujo, R. C., Baltatu, O., Oliveira, S. M., Tschope, C., Fink, E., Hoffmann, S., Plehm, R., Chai, K. X., Chao, L., *et al.* (2000) *FASEB J.* **14,** 1858–1860.

20. van Leeuwen, B. H., Evans, B. A., Tregear, G. W. & Richards, R. I. (1986) *J. Biol. Chem.* **261,** 5529–5535.

21. Meneton, P., Schultheis, P. J., Greeb, J., Nieman, M. L., Liu, L. H., Clarke, L. L., Duffy, J. J., Doetschman, T., Lorenz, J. N. & Shull, G. E. (1998) *J. Clin. Invest.* **101,** 536–542.

22. Church, G. M. & Gilbert, W. (1984) *Proc. Natl. Acad. Sci. USA* **81,** 1991–1995.

23. Orfila, C., Bascands, J. L., Suc, J. M. & Girolami, J. P. (1988) *J. Histochem. Cytochem.* **36,** 1463–1469.

24. Alhenc-Gelas, F., Marchetti, J., Allegrini, J., Corvol, P. & Menard, J. (1981) *Biochim. Biophys. Acta* **677,** 477–488.

25. Nussberger, J., Cugno, M., Amstutz, C., Cicardi, M., Pellacani, A. & Agostoni, A. (1998) *Lancet* **351,** 1693–1697.

26. Chevalier, B., Heudes, D., Heymes, C., Basset, A., Dakhli, T., Bansard, Y., Jouquey, S., Hamon, G., Bruneval, P., Swynghedauw, B. & Carre, F. (1995) *Circulation* **92,** 1947–1953.

27. Scorsin, M., Hagege, A. A., Dolizy, I., Marotte, F., Mirochnik, N., Copin, H., Barnoux, M., le Bert, M., Samuel, J. L., Rappaport, L. & Menasche, P. (1998) *Circulation* **98,** 151–156.

28. Murphy, A. M., Kogler, H., Georgakopoulos, D., McDonough, J. L., Kass, D. A., Van Eyk, J. E. & Marban, E. (2000) *Science* **287,** 488–491.

29. Guenoun, T., Montagne, O., Laplace, M. & Crozatier, B. (2000) *Anesthesiology* **92,** 542–549.

30. Henrion, D., Terzi, F., Matrougui, K., Duriez, M., Boulanger, C. M., Colucci-Guyon, E., Babinet, C., Briand, P., Friedlander, G., Poitevin, P. & Levy, B. I. (1997) *J. Clin. Invest.* **100,** 2909–2914.

31. Clements, J. A. (1989) *Endocr. Rev.* **10,** 393–419.

32. Evans, B. A., Drinkwater, C. C. & Richards, R. I. (1987) *J. Biol. Chem.* **262,** 8027–8034.

33. Alfie, M. E., Sigmon, D. H., Pomposiello, S. I. & Carretero, O. A. (1997) *Hypertension* **29,** 483–487.

34. Madeddu, P., Varoni, M. V., Palomba, D., Emanueli, C., Demontis, M. P., Glorioso, N., Dessi-Fulgheri, P., Sarzani, R. & Anania, V. (1997) *Circulation* **96,** 3570–3578.

35. Rupniak, N. M., Boyce, S., Webb, J. K., Williams, A. R., Carlson, E. J., Hill, R. G., Borkowski, J. A. & Hess, J. F. (1997) *Pain* **71,** 89–97.

36. Alfie, M. E., Alim, S., Mehta, D., Shesely, E. G. & Carretero, O. A. (1999) *Hypertension* **33,** 1436–1440.

37. Pesquero, J. B., Araujo, R. C., Heppenstall, P. A., Stucky, C. L., Silva, J. A., Jr., Walther, T., Oliveira, S. M., Pesquero, J. L., Paiva, A. C., Calixto, J. B., *et al.* (2000) *Proc. Natl. Acad. Sci. USA* **97,** 8140–8145. (First Published June 20, 2000; 10.1073/pnas.120035997)

38. Elliot, A. & Nuzum, F. (1934) *Endocrinology* **18,** 462–474.

39. Geisterfer-Lowrance, A. A., Christe, M., Conner, D. A., Ingwall, J. S., Schoen, F. J., Seidman, C. E. & Seidman, J. G. (1996) *Science* **272,** 731–734.

40. Arber, S., Hunter, J. J., Ross, J., Jr., Hongo, M., Sansig, G., Borg, J., Perriard, J. C., Chien, K. R. & Caroni, P. (1997) *Cell* **88,** 393–403.

41. McConnell, B. K., Jones, K. A., Fatkin, D., Arroyo, L. H., Lee, R. T., Aristizabal, O., Turnbull, D. H., Georgakopoulos, D., Kass, D., Bond, M., *et al.* (1999) *J. Clin. Invest.* **104,** 1235–1244.

42. Baig, M. K., Goldman, J. H., Caforio, A. L., Coonar, A. S., Keeling, P. J. & McKenna, W. J. (1998) *J. Am. Coll. Cardiol.* **31,** 195–201.

43. Mestroni, L., Rocco, C., Gregori, D., Sinagra, G., Di Lenarda, A., Miocic, S., Vatta, M., Pinamonti, B., Muntoni, F., Caforio, A. L., *et al.* (1999) *J. Am. Coll. Cardiol.* **34,** 181–190.

44. Bonne, G., Carrier, L., Richard, P., Hainque, B. & Schwartz, K. (1998) *Circ. Res.* **83,** 580–593.

45. Chien, K. R. (1999) *Cell* **98,** 555–558.

46. Bergaya, S., Meneton, P., Bloch-Faure, M., Mathieu, E., Alhenc-Gelas, F., Levy, B. & Boulanger, C. (2001) *Circ. Res.*, in press.

47. Ritchie, R. H., Marsh, J. D., Lancaster, W. D., Diglio, C. A. & Schiebinger, R. J. (1998) *Hypertension* **31,** 39–44.

48. Emanueli, C., Maestri, R., Corradi, D., Marchione, R., Minasi, A., Tozzi, M. G., Salis, M. B., Straino, S., Capogrossi, M. C., Olivetti, G. & Madeddu, P. (1999) *Circulation* **100,** 2359–2365.